Equilibration properties of small quantum systems: further examples

J. M. Luck

Equilibration properties of small quantum systems: further examples

J M Luck

Institut de Physique Théorique, Université Paris-Saclay, CEA and CNRS, 91191 Gif-sur-Yvette, France

Abstract. It has been proposed to investigate the equilibration properties of a small isolated quantum system by means of the matrix of asymptotic transition probabilities in some preferential basis. The trace T of this matrix measures the degree of equilibration of the system prepared in a typical state of the preferential basis. This quantity may vary between unity (ideal equilibration) and the dimension N of the Hilbert space (no equilibration at all). Here we analyze several examples of simple systems where the behavior of T can be investigated by analytical means. We first study the statistics of T when the Hamiltonian governing the dynamics is random and drawn from a distribution invariant under the group $\mathrm{U}(N)$ or $\mathrm{O}(N)$. We then investigate a quantum spin S in a tilted magnetic field making an arbitrary angle with the preferred quantization axis, as well as a tight-binding particle on a finite electrified chain. The last two cases provide examples of the interesting situation where varying a system parameter – such as the tilt angle or the electric field – through some scaling regime induces a continuous transition from good to bad equilibration properties.

E-mail: jean-marc.luck@cea.fr

1. Introduction

The last decade has witnessed an immense activity around the themes of thermalization and equilibration in isolated quantum systems (see [1, 2, 3, 4, 5, 6] for comprehensive reviews). This renewed interest in an old classic subject of Quantum Mechanics was mostly triggered by progress on the experimental side in cold-atom physics. The physical mechanisms underling equilibration and thermalization are far from obvious. On the one hand, an isolated quantum system evolves by some unitary dynamics, and therefore keeps the memory of its initial state. On the other hand, if the system is large enough, concepts from Statistical Mechanics can be expected to apply at least approximately. Most recent works have dealt with large many-body quantum systems, the key issues including the description of a small subsystem by a thermodynamical ensemble (either microcanonical or canonical), the thermalization properties of single highly-excited states, and the role of conservation laws and of integrability.

An alternative and complementary viewpoint, where the main focus is on the unitary evolution of a small quantum system considered as a whole, has been emphasized in [7]. There, the key quantity is the matrix Q of asymptotic transition probabilities in some preferential basis. The trace T of this matrix is also the sum of the inverse participation ratios of all eigenstates of the Hamiltonian in the same basis. This quantity has been put forward as a measure of the degree of equilibration of the full system if launched from a typical basis state. This line of thought has been illustrated by means of a detailed study of a single tight-binding particle on a finite segment of N sites in a random potential [7]. The main findings concern the regime of a weak disorder, where T exhibits a finite value $T = T^{(0)} \approx 3/2$ in the ballistic regime, testifying good equilibration, a linear growth with the sample size ($T \approx NQ$) in the localized regime, testifying poor equilibration, and a universal scaling law of the form

$$T \approx T^{(0)} + \frac{1}{N}\,\Phi\big(Nw^{2/3}\big), \tag{1.1}$$

interpolating between both above regimes, where w is the strength of the disorder, and the crossover exponent $2/3$ is related to the anomalous scaling of the most localized band-edge states. The behavior of T in a clean quantum many-body system has then been considered in [8], where the statistics of inverse participation ratios in the XXZ spin chain with anisotropy parameter Δ has been investigated numerically. There, the quantity T was found to grow linearly with the system size ($T \sim L$) in the gapless phase of the model ($|\Delta| < 1$), and exponentially ($T \sim \exp(aL)$) in the gapped phase ($|\Delta| > 1$). The inverse participation ratios in the XX spin chain ($\Delta = 0$), which can be mapped onto a free-fermion problem, have been investigated more recently in [9]. The partial results obtained there attest the difficulty of any analytical progress in this area.

In this paper we analyse in detail several other examples of simple quantum systems for which the behavior of the quantity T can be investigated by analytical means. Section 2 provides a reminder of the transition matrix formalism proposed in [7], emphasizing the role and the meaning of T. In section 3 we investigate the statistics of T corresponding to a random Hamiltonian whose distribution is invariant under the group $\mathrm{U}(N)$ or $\mathrm{O}(N)$, thus keeping in line with the random matrix theory approach to quantum chaos. Section 4 deals with a single quantum spin S submitted to a tilted magnetic field making an angle θ with respect to the quantization axis defining the preferred basis. Finally, the case of a tight-binding particle on a finite electrified

chain is considered in section 5. This situation is somehow a deterministic analogue of the case considered in [7], where the ladder of Wannier-Stark states replaces Anderson localized states. It is however richer, as it features two successive scaling regimes in the small-field region. Our findings are summarized and discussed in section 6.

2. A reminder on the transition matrix formalism

This section provides a reminder of the transition matrix formalism which has been proposed in [7] to describe equilibration in small isolated quantum systems. Consider a system whose Hilbert space has dimension N. Let $\{|a\rangle\}$ $(a = 1, \ldots, N)$ be a preferential basis, chosen once for all. In that basis the Hamiltonian $\mathcal{H}$ is some $N \times N$ matrix. We assume that its eigenvalues E_n are non-degenerate.

If the system is launched in one of the basis states, say $|a\rangle$, the probability for it to be in state $|b\rangle$ at a subsequent time t reads

$$P_{ab}(t) = \sum_{m,n} \mathrm{e}^{\mathrm{i}(E_n - E_m)t} \langle b|m\rangle\langle m|a\rangle\langle a|n\rangle\langle n|b\rangle, \tag{2.1}$$

where $\{|n\rangle\}$ $(n = 1, \ldots, N)$ is a basis of normalized eigenstates, such that $\mathcal{H}|n\rangle = E_n|n\rangle$. The stationary state reached by the system is characterized by the time-averaged transition probabilities

$$Q_{ab} = \lim_{t\to\infty} \frac{1}{t} \int_0^t P_{ab}(t')\,\mathrm{d}t'. \tag{2.2}$$

In the absence of spectral degeneracies, we have

$$Q_{ab} = \sum_n |\langle a|n\rangle|^2\ |\langle b|n\rangle|^2. \tag{2.3}$$

The transition matrix Q is the central object of this formalism. Let us begin with a few general properties. The matrix Q only depends on the eigenstates $|n\rangle$ of the Hamiltonian $\mathcal{H}$, and not on its eigenvalues E_n. Therefore, any two Hamiltonians with the same eigenstate basis share the same matrix Q, irrespective of their spectra. In full generality, the matrix Q reads

$$Q = RR^T, \tag{2.4}$$

where the matrix R is given by

$$R_{an} = |\langle a|n\rangle|^2, \tag{2.5}$$

and R^T is its transpose. The matrix Q is therefore real symmetric and positive definite. The matrix R is real, albeit not symmetric in general; it may therefore have complex spectrum. Finally, both matrices Q and R are doubly stochastic: their row and column sums equal unity

$$\sum_a R_{an} = \sum_n R_{an} = \sum_a Q_{ab} = \sum_b Q_{ab} = 1. \tag{2.6}$$

More generally, one can associate real matrices Q and R obeying the above properties with any pair of orthonormal bases $\{|a\rangle\}$ and $\{|n\rangle\}$, related to each other by an arbitrary unitary transformation U such that

$$U_{an} = \langle a|n\rangle. \tag{2.7}$$

Coming back to equilibration properties, the diagonal element

$$Q_{aa} = \sum_n |\langle a|n\rangle|^4, \tag{2.8}$$

i.e., the stationary return probability to the basis state $|a\rangle$, can be recast as

$$Q_{aa} = \mathrm{tr}\, \omega_a^2, \tag{2.9}$$

where

$$\omega_a = \sum_n |\langle a|n\rangle|^2 \; |n\rangle\langle n| \tag{2.10}$$

is the stationary density matrix issued from state $|a\rangle$. The right-hand side of (2.9) is called the purity of ω_a. Its reciprocal, i.e.,

$$d_a = \frac{1}{Q_{aa}}, \tag{2.11}$$

provides a measure of the dimension of the subspace of Hilbert space where the system equilibrates if launched from state $|a\rangle$ [10, 11, 12, 13, 14, 15].

The equilibration properties of the system launched from a typical basis state are encoded in the trace of the matrix Q:

$$T = \sum_{a,n} |\langle a|n\rangle|^4 = \sum_a Q_{aa} = \sum_n I_n, \tag{2.12}$$

where

$$I_n = \sum_a |\langle a|n\rangle|^4 \tag{2.13}$$

is the inverse participation ratio (IPR) [16, 17, 18, 19] of the eigenstate $|n\rangle$ of $\mathcal{H}$ in the preferential basis. The return probabilities Q_{aa} and the IPR I_n therefore somehow appear as dual to each other.

The ratio

$$D = \frac{N}{T} \tag{2.14}$$

is such that

$$\frac{1}{D} = \frac{1}{N} \sum_a \frac{1}{d_a}. \tag{2.15}$$

Hence D provides a measure of the dimension of the subspace which hosts the equilibration dynamics for a typical initial state. The trace T and the effective dimension D are always between the following extremal values.

Ideal equilibration. If the eigenstates of $\mathcal{H}$ are uniformly spread over the preferential basis, we have

$$R_{an} = \frac{1}{N} \tag{2.16}$$

for all a and n. The bases $\{|a\rangle\}$ and $\{|n\rangle\}$ are said to be mutually unbiased [20, 21, 22]. Hence

$$Q_{ab} = \frac{1}{N} \tag{2.17}$$

for all a and b, and

$$T_{\min} = 1, \qquad D_{\max} = N. \tag{2.18}$$

This ideal situation corresponds to a perfectly equilibrated stationary state, with no memory of the initial state at all.

No equilibration. This situation is the exact opposite of the previous one. If $\mathcal{H}$ is diagonal in the preferential basis, its eigenstates $|n\rangle$ can be ordered so as to have

$$R_{an} = \delta_{an} \tag{2.19}$$

for all a and n, and

$$Q_{ab} = \delta_{ab} \tag{2.20}$$

for all a and b, δ being the Kronecker symbol, and so

$$T_{\max} = N, \qquad D_{\min} = 1. \tag{2.21}$$

In such a situation, the system keeps a full memory of its initial state, and so there is no equilibration at all.

3. Random matrix theory approach

Let us first investigate the statistics of T obtained by choosing the Hamiltonian matrix $\mathcal{H}$ at random. Keeping in line with the random matrix theory approach to quantum chaos, which has been used extensively to investigate many properties of complex quantum systems, ranging from energy spectra to transport properties [23, 24, 25, 26], we assume that the distribution of $\mathcal{H}$ is invariant under the action of a suitable chosen symmetry group, here $\mathrm{U}(N)$ or $\mathrm{O}(N)$. This line of thought implies in particular that the distribution of the eigenstates of $\mathcal{H}$ shows no preferred direction. More precisely, the matrix U encoding the eigenstates of $\mathcal{H}$ in the preferred basis, introduced in (2.7), is distributed according to the Haar measure on the appropriate symmetry group. It will be sufficient to consider the first two cumulants of T, i.e., the mean value $\langle T\rangle$ and the variance $\mathrm{var}\, T = \langle T^2\rangle - \langle T\rangle^2$.

The unitary case. We consider first the situation where the Hamiltonian $\mathcal{H}$ is an $N \times N$ complex Hermitian matrix. The relevant symmetry group is then the unitary group $\mathrm{U}(N)$. We have

$$\langle T\rangle_{\mathrm{U}} = N^2 A_{\mathrm{U}}, \tag{3.1}$$

$$(\mathrm{var}\, T)_{\mathrm{U}} = N^2 \left(B_{\mathrm{U}} + 2(N-1)C_{\mathrm{U}} + (N-1)^2 D_{\mathrm{U}} - N^2 A_{\mathrm{U}}^2\right), \tag{3.2}$$

with

$$\begin{array}{ll} A_{\mathrm{U}} = \langle |U_{11}|^4\rangle_{\mathrm{U}}, & B_{\mathrm{U}} = \langle |U_{11}|^8\rangle_{\mathrm{U}}, \\ C_{\mathrm{U}} = \langle |U_{11}|^4 |U_{12}|^4\rangle_{\mathrm{U}}, & D_{\mathrm{U}} = \langle |U_{11}|^4 |U_{22}|^4\rangle_{\mathrm{U}}, \end{array} \tag{3.3}$$

where $\langle \ldots\rangle_{\mathrm{U}}$ denotes an average with respect to the normalized Haar measure on $\mathrm{U}(N)$.

Moments of this kind have attracted much attention in the past, and several approaches have been proposed to evaluate them [27, 28, 29, 30, 31, 32, 33, 34, 35, 36]. Table 1 gives the values of the moments A_{U}, B_{U}, C_{U} and D_{U} for the unitary group $\mathrm{U}(N)$ (see (3.3)) and A_{O}, B_{O}, C_{O} and D_{O} for the orthogonal group $\mathrm{O}(N)$ (see (3.8)).

Using the results of table 1, we obtain

$$\langle T\rangle_{\mathrm{U}} = \frac{2N}{N+1}, \tag{3.4}$$

$$(\mathrm{var}\, T)_{\mathrm{U}} = \frac{4(N-1)}{(N+1)^2(N+3)}. \tag{3.5}$$

U(N)	O(N)
$A_{\rm U} = \frac{2}{N(N+1)}$	$A_{\rm O} = \frac{3}{N(N+2)}$
$B_{\rm U} = \frac{24}{N(N+1)(N+2)(N+3)}$	$B_{\rm O} = \frac{105}{N(N+2)(N+4)(N+6)}$
$C_{\rm U} = \frac{4}{N(N+1)(N+2)(N+3)}$	$C_{\rm O} = \frac{9}{N(N+2)(N+4)(N+6)}$
$D_{\rm U} = \frac{4}{N^2(N-1)(N+3)}$	$D_{\rm O} = \frac{9(N+3)(N+5)}{N(N^2-1)(N+2)(N+4)(N+6)}$

Table 1. Values of the integrals A, B, C and D for both symmetry classes. For the unitary group U(N) (see (3.3)), the one-vector integrals $A_{\rm U}$, $B_{\rm U}$ and $C_{\rm U}$ are given in [27, 36] while the two-vector integral $D_{\rm U}$, given in [34], can be checked using the recursive approach of [36]. For the orthogonal group O(N) (see (3.8)), the one-vector integrals $A_{\rm O}$, $B_{\rm O}$ and $C_{\rm O}$ are given in [36], and the two-vector integral $D_{\rm O}$, given in [35], can again be checked using [36].

The orthogonal case. We now turn to the situation where the dynamics is invariant under time reversal, so that the Hamiltonian $\mathcal{H}$ is a real symmetric matrix. The relevant symmetry group is then the orthogonal group O(N). We have

$$\langle T\rangle_{\rm O} = N^2 A_{\rm O}, \tag{3.6}$$

$$({\rm var}\ T)_{\rm O} = N^2\left(B_{\rm O} + 2(N-1)C_{\rm O} + (N-1)^2 D_{\rm O} - N^2 A_{\rm O}^2\right), \tag{3.7}$$

with

$$\begin{array}{ll} A_{\rm O} = \langle \Omega_{11}^4\rangle_{\rm O}, & B_{\rm O} = \langle \Omega_{11}^8\rangle_{\rm O}, \\ C_{\rm O} = \langle \Omega_{11}^4 \Omega_{12}^4\rangle_{\rm O}, & D_{\rm O} = \langle \Omega_{11}^4 \Omega_{22}^4\rangle_{\rm O}, \end{array} \tag{3.8}$$

where $\langle\ldots\rangle_{\rm O}$ now denotes an average with respect to the normalized Haar measure on O(N). Using again the results of table 1, we obtain

$$\langle T\rangle_{\rm O} = \frac{3N}{N+2}, \tag{3.9}$$

$$({\rm var}\ T)_{\rm O} = \frac{24N(N-1)}{(N+1)(N+2)^2(N+6)}. \tag{3.10}$$

For a very large dimension N, T converges to the limits

$$T_{\rm U} = 2, \qquad T_{\rm O} = 3, \tag{3.11}$$

which only depend on the symmetry class of the Hamiltonian. These finite values testify extended eigenstates and good equilibration properties, as could be expected for a generic Hamiltonian. The limit values (3.11) are deterministic, in the sense that fluctuations of individual values of T become negligible for large N, as testified by the $1/N^2$ falloff of the variances

$$({\rm var}\ T)_{\rm U} \approx \frac{4}{N^2}, \qquad ({\rm var}\ T)_{\rm O} \approx \frac{24}{N^2}. \tag{3.12}$$

The limit values (3.11) coincide with the outcome of the following naive approach. In the unitary case, consider T as the sum of N^2 independent quantities of the form $|u|^4$, modeling the entries u as centered complex Gaussian variables such that $\langle|u|^2\rangle = 1/N$. This yields $T_{\rm U} = N^2\langle|u|^4\rangle = \langle|u|^4\rangle/\langle|u|^2\rangle^2 = 2$. Similarly, in the orthogonal case, consider T as the sum of N^2 independent quantities of the form ω^4, modeling the entries ω as real Gaussian variables such that $\langle\omega^2\rangle = 1/N$. This

yields $T_{\rm O} = N^2\langle\omega^4\rangle = \langle\omega^4\rangle/\langle\omega^2\rangle^2 = 3$. In the same vein, the $1/N^2$ decay of the variances (3.12) also conforms with the above naive approach, viewing T as the sum of N^2 independent random variables.

For finite values of N (see figure 1), the results (3.4), (3.5) and (3.9), (3.10) have a simple rational dependence on N. The mean values $\langle T\rangle$ increase monotonically from unity and saturate to the limits (3.11). The variances vanish both for $N = 1$ and $N \to \infty$, and therefore present a maximum. The maximum of $(\text{var } T)_{\rm U}$, equal to $4/45$, is reached for $N = 2$, while the maximum of $(\text{var } T)_{\rm O}$, equal to $4/25$, is reached for $N = 3$ and 4.

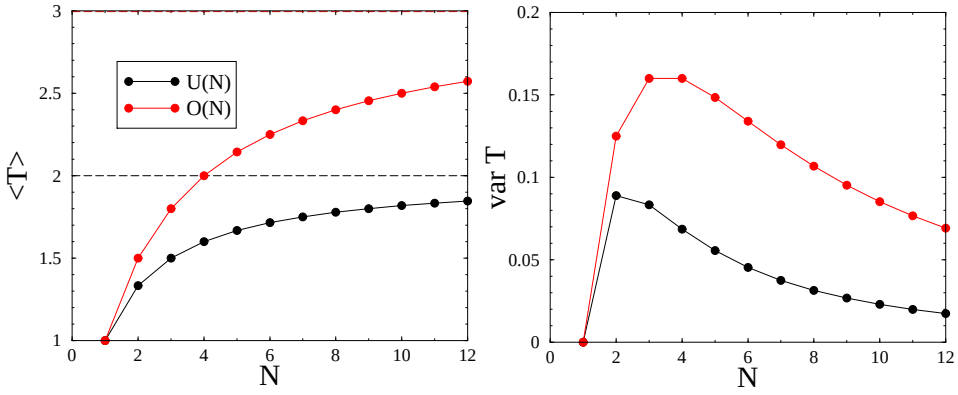

Figure 1. Mean values (left) and variances (right) of T, for a random Hamiltonian with a distribution invariant under the unitary group U(N) (see (3.4), (3.5)) or the orthogonal group O(N) (see (3.9), (3.10)). Dashed horizontal lines in left panel: large-N limits $T_{\rm U} = 2$, $T_{\rm O} = 3$ (see (3.11)).

4. A spin in a tilted magnetic field

This section is devoted to the dynamics of a single quantum spin in the representation of SU(2) of dimension

$$N = 2S + 1. \tag{4.1}$$

The spin S is either an integer (if N is odd) or a half-integer (if N is even). We choose the z-axis as preferred quantization axis. The preferred basis thus consists of the eigenstates $|a\rangle$ of S_z, where a takes the N values $a = -S, \ldots, S$, with unit steps. The spin is subjected to a tilted external magnetic field $\mathbf{h}$ making an angle θ with the z-axis, with $0 \le \theta \le \pi$. The corresponding Hamiltonian reads, in dimensionless units

$$\mathcal{H} = \cos\theta\, S_z + \sin\theta\, S_x. \tag{4.2}$$

The spin S and the tilt angle θ are the two parameters of the model.

4.1. The simplest case: $S = \frac{1}{2}$

Let us consider first the case of a spin $S = \frac{1}{2}$, so that $N = 2$. The Hamiltonian

$$\mathcal{H} = \frac{1}{2}\begin{pmatrix} \cos\theta & \sin\theta \\ \sin\theta & -\cos\theta \end{pmatrix} \tag{4.3}$$

has eigenvalues $E_\pm = \pm\frac{1}{2}$. The matrix encoding the corresponding eigenstates is

$$U = \begin{pmatrix} \cos\frac{\theta}{2} & \sin\frac{\theta}{2} \\ -\sin\frac{\theta}{2} & \cos\frac{\theta}{2} \end{pmatrix}, \tag{4.4}$$

up to arbitrary phases. The matrices R and Q (see (2.3), (2.5)) therefore read

$$R = \frac{1}{2}\begin{pmatrix} 1+\cos\theta & 1-\cos\theta \\ 1-\cos\theta & 1+\cos\theta \end{pmatrix}, \tag{4.5}$$

$$Q = \frac{1}{2}\begin{pmatrix} 1+\cos^2\theta & 1-\cos^2\theta \\ 1-\cos^2\theta & 1+\cos^2\theta \end{pmatrix}. \tag{4.6}$$

We notice that the matrices U and R are respectively orthogonal and symmetric. We have finally

$$T = 1 + \cos^2\theta. \tag{4.7}$$

4.2. The general case

In the general case (S arbitrary), the eigenvalues of $\mathcal{H}$ are $E_n = n = -S, \ldots, S$, again with unit steps. The matrix U encoding the corresponding eigenstates in the preferred basis is nothing but the Wigner 'small' rotation matrix $d^{(S)}(\theta)$, describing the transformation of a spin S under a rotation of angle θ around the y-axis. References [37, 38, 39, 40] give a full account of its properties. The rotation matrix $d^{(S)}(\theta)$ is a real orthogonal matrix, whose entries obey the symmetry property

$$d^{(S)}_{a,n}(\theta) = (-1)^{a-n} d^{(S)}_{-a,-n}(\theta). \tag{4.8}$$

This identity allows us to recast the entries of the matrix R as

$$R_{an} = (-1)^{a-n} d^{(S)}_{a,n}(\theta) d^{(S)}_{-a,-n}(\theta). \tag{4.9}$$

Expanding the product of rotation matrix elements over irreducible representations [37, 38, 39, 40], we obtain

$$R_{an} = \sum_{j=0}^{N-1} \varphi^{(j)}_a \varphi^{(j)}_n P_j(\cos\theta). \tag{4.10}$$

In this expression, the integer j takes $N = 2S+1$ values,

$$P_j(\cos\theta) = d^{(j)}_{0,0}(\theta) \tag{4.11}$$

are the Legendre polynomials, and

$$\varphi^{(j)}_n = (-1)^n \langle S, n, S, -n | j, 0\rangle \tag{4.12}$$

are Clebsch-Gordan coefficients, up to signs.

The identity (4.10) has several consequences. First, it shows that R is a real symmetric matrix. The properties that U and R are respectively orthogonal and symmetric, already observed for $S = \frac{1}{2}$, thus hold for an arbitrary spin S. Furthermore, (4.10) yields the spectral decomposition of the matrix R: $r_j = P_j(\cos\theta)$ are its eigenvalues, with the corresponding normalized eigenvectors $\varphi^{(j)}_n$ being independent of the angle θ. Finally, the matrix R being symmetric, (2.4) implies $Q = R^2$, and so the eigenvalues of Q are $q_j = r_j^2$. We thus obtain the explicit formula

$$T = \sum_{j=0}^{N-1} P_j^2(\cos\theta). \tag{4.13}$$

Here are a few immediate properties of the above expression. First, it is invariant when changing θ to $\pi - \theta$, as should be. The Legendre polynomials indeed obey the symmetry property $P_j(-x) = (-1)^j P_j(x)$, so that T is an even function of $x = \cos\theta$. For $\theta = 0$ or $\theta = \pi$, we have exactly $T = N$. The Hamiltonian indeed reads $\mathcal{H} = \pm S_z$, and so its eigenstates coincide with the preferred basis. This is one example of the situation referred to in section 2 as *no equilibration*. For $S = \frac{1}{2}$, i.e., $N = 2$, the result (4.7) is recovered, as $P_0(x) = 1$ and $P_1(x) = x$.

Figure 2 shows the product $T \sin\theta$ against the reduced tilt angle θ/π, for N ranging from 2 to 20. The rationale behind the plotted quantity is the growth law (4.20).

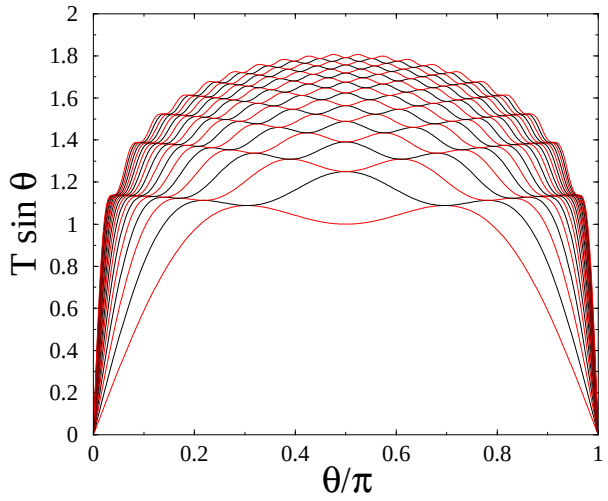

Figure 2. Product $T \sin\theta$ against θ/π for N ranging from 2 to 20 (bottom to top). Black curves: integer spin S (N odd). Red curves: half-integer spin S (N even). The lowest curve corresponds to $S = \frac{1}{2}$ (see (4.7)).

4.3. Behavior at large N (semi-classical regime)

The goal of this section is to estimate the growth law of T in the semi-classical regime of large values of N. The quantity T is clearly an increasing function of N, at fixed angle θ, as the expression (4.13) is a sum of positive terms.

Consider first the mean value $\langle T \rangle$, assuming that the magnetic field $\mathbf{h}$ acting on the spin is isotropically distributed. This amounts to $x = \cos\theta$ being uniformly distributed in the range $-1 \leq x \leq 1$. The identity (see e.g. [41, Vol. II, Ch. 10])

$$\int_{-1}^{1} P_j^2(x)\,\mathrm{d}x = \frac{2}{2j+1} \tag{4.14}$$

yields

$$\langle T \rangle = \sum_{j=0}^{N-1} \frac{1}{2j+1} = H_{2N} - \tfrac{1}{2} H_N, \tag{4.15}$$

where H_N are the harmonic numbers, and hence

$$\langle T\rangle \approx \frac{1}{2}\ln(4\mathrm{e}^{\gamma}N), \tag{4.16}$$

where $\gamma = 0.577\,215\ldots$ is Euler's constant. The mean value $\langle T\rangle$ therefore grows logarithmically with N.

A similar logarithmic growth holds at any fixed value of the tilt angle θ. This can be shown by means of the generating series [42, 43, 44]

$$\sum_{j\geq 0} P_j^2(\cos\theta)\, z^j = \frac{2}{\pi(1-z)}\,\mathbf{K}(k), \qquad k^2 = -\frac{4z\sin^2\theta}{(1-z)^2}, \tag{4.17}$$

where $\mathbf{K}(k)$ is the complete elliptic integral of the first kind. We are interested in the singular behavior of the above expression as $z\to 1$. As the modulus k diverges in that limit, it is advantageous to change the square modulus [41, Vol. II, Ch. 13] from k^2 to

$$q^2 = -\frac{k^2}{1-k^2} = \frac{4z\sin^2\theta}{(1-z)^2+4z\sin^2\theta}. \tag{4.18}$$

We have then $\mathbf{K}(k) = q'\,\mathbf{K}(q)$, with $q' = \sqrt{1-q^2}$. Furthermore, as $q\to 1$, i.e., $q'\to 0$, the new elliptic integral diverges as $\mathbf{K}(q)\approx \ln(4/q')$, so that

$$\sum_{j\geq 0} P_j(\cos\theta)^2\, z^j \approx \frac{1}{\pi\sin\theta}\ln\frac{8\sin\theta}{1-z}, \tag{4.19}$$

and finally

$$T \approx \frac{1}{\pi\sin\theta}\ln(8\mathrm{e}^{\gamma}N\sin\theta). \tag{4.20}$$

The quantity T thus grows logarithmically in N for any fixed value of the angle θ, with an angle-dependent amplitude $1/(\pi\sin\theta)$. Hence the product $T\sin\theta$, plotted in figure 2, grows as $(1/\pi)\ln N$, to leading order, irrespective of θ. Finally, the growth law (4.16) of the mean value $\langle T\rangle$ can be recovered by integrating (4.20) over $0\leq\theta\leq\pi$ with the measure $\frac{1}{2}\sin\theta\,\mathrm{d}\theta$.

4.4. Scaling behavior at small angle

The quantity T obeys a non-trivial scaling behavior in the regime where N is large and the tilt angle θ is small, interpolating between the growth laws $T = T_{\max} = N$ for $\theta = 0$ and $T\sim\ln N$ for any non-zero θ (see (4.20)).

This scaling behavior is inherited from the scaling formula obeyed by the Legendre polynomials for j large and θ small, sometimes referred to as Hilb's formula (see e.g. [41, Vol. II, Ch. 10]), i.e.,

$$P_j(\cos\theta)\approx J_0(s), \tag{4.21}$$

with

$$s = j\theta \tag{4.22}$$

and J_0 being the Bessel function. Inserting this into (4.13), we obtain the scaling law

$$T\approx NF(u), \tag{4.23}$$

or, equivalently,

$$T\theta\approx G(u), \tag{4.24}$$

with

$$u = N\theta \tag{4.25}$$

and

$$G(u) = uF(u) = \int_0^u J_0^2(s)\,\mathrm{d}s. \tag{4.26}$$

The formula (4.23) is more adapted to small values of the scaling variable u. The function $F(u)$ decreases monotonically from $F(0) = 1$ to zero. For small u, the expansion

$$F(u) = 1 - \frac{u^2}{6} + \cdots \tag{4.27}$$

matches the exact small-angle expansion

$$T = N - \frac{N(N^2-1)}{6}\,\theta^2 + \cdots \tag{4.28}$$

of the full expression (4.13). We have $F(u) = 1/2$ for $u \approx 2.277$, so that T drops from its maximal value $T = N$ at $\theta = 0$ to $T = N/2$ for $\theta \approx 2.277/N$.

The formula (4.24) is more adapted to large values of u. The function $G(u)$ is monotonically increasing. It exhibits an infinite sequence of 'pauses' at the zeros j_n of the Bessel function J_0, with heights $G(j_n) = G_n$, around which it varies cubically, as $G(u) - G_n \sim (u - j_n)^3$. The asymptotic behavior of the Bessel function

$$J_0(s) \approx \left(\frac{2}{\pi s}\right)^{1/2} \cos\left(s - \frac{\pi}{4}\right) \qquad (s \to \infty) \tag{4.29}$$

implies that $G(u)$ grows logarithmically for large u, as

$$G(u) \approx \frac{1}{\pi} \ln(8\mathrm{e}^{\gamma} u), \tag{4.30}$$

where the finite part has been obtained by matching with (4.20). The zeros read approximately $j_n \approx n\pi$, so that the heights of the pauses also grow logarithmically, as

$$G_n \approx \frac{1}{\pi} \ln(8\pi\mathrm{e}^{\gamma} n). \tag{4.31}$$

There are 12 pauses with height less than 2, and 277 pauses with height less than 3. The first of these pauses predict the heights of the ripples which are visible on the data for finite values of N, shown in figure 2.

Figure 3 shows the above scaling functions. The left panel shows the function $F(u)$ entering (4.23). The right panel shows the function $G(u) = uF(u)$ entering (4.24). Blue symbols show the first three pauses.

5. A tight-binding particle on an electrified chain

In this section we investigate a tight-binding particle on a finite chain of N sites subjected to a uniform electric field F. We assume $F > 0$ for definiteness.

The preferential basis consists of the Wannier states $|a\rangle$ associated with the sites of the chain ($a = 1, \ldots, N$). In terms of the amplitudes $\psi_a = \langle a|\psi\rangle$, the eigenvalue equation $\mathcal{H}\psi = E\psi$ reads

$$\psi_{a+1} + \psi_{a-1} + \left(a - \frac{N+1}{2}\right) F\psi_a = E\psi_a, \tag{5.1}$$

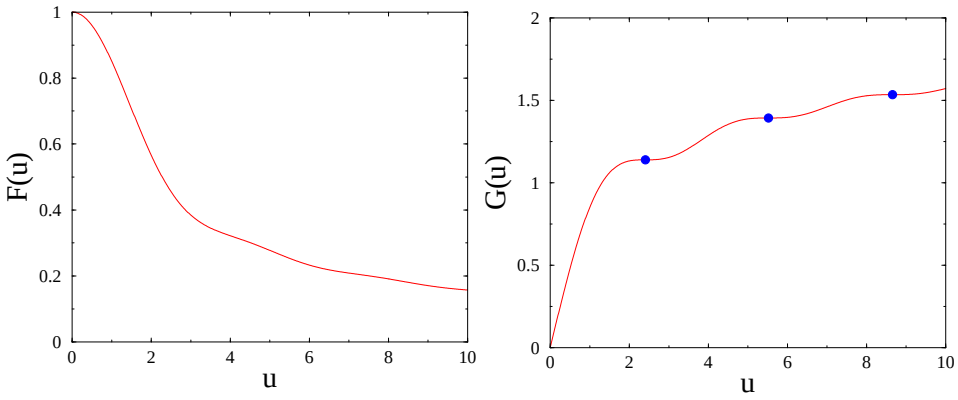

Figure 3. The functions $F(u)$ (left) and $G(u) = uF(u)$ (right), respectively entering the scaling laws (4.23) and (4.24), against $u = N\theta$. Blue symbols on the right panel: first three pauses at heights $G_1 \approx 1.13861$, $G_2 \approx 1.39251$, $G_3 \approx 1.53384$ (see text).

in reduced units, where the dimensionless electric field F equals the potential drop across one unit cell, in units of the hopping rate.

We shall consider an open chain with Dirichlet boundary conditions ($\psi_0 = \psi_{N+1} = 0$). The choice of the constant offset in the electrostatic potential

$$V_a = \left(\frac{N+1}{2} - a\right) F \tag{5.2}$$

ensures that the latter vanishes in the middle of the sample. As a consequence, the energy spectrum is symmetric with respect to $E = 0$. Indeed, if the wavefunction ψ_a describes a state with energy E, then $(-1)^a \psi_{N+1-a}$ describes a state with energy $-E$. Both states have the same IPR. In particular, samples with odd sizes N have a single non-degenerate eigenstate at $E = 0$.

The problem of an electron in a uniform electric field is an old classic of Quantum Mechanics. The spectrum of a tight-binding particle on the infinite chain has been known for long [45, 46, 47]. It consists of an infinite sequence of localized states, the corresponding energies having a constant spacing ($\Delta E = F$ in our reduced units). Such a discrete spectrum has been dubbed a Wannier-Stark ladder [48, 49, 50]. The fate of these ladders on finite samples has been investigated by several authors in the 1970s [51, 52, 53, 54, 55, 56]. In order to investigate the behavior of T in the various regimes of system size N and applied electric field F, we have to thoroughly revisit these works.

5.1. General approach

A general approach consists in solving (5.1) for an arbitrary value of the energy E, imposing the boundary conditions $\psi_0 = 0$ and $\psi_1 = 1$. This yields

$$\begin{aligned} \psi_2 &= E + \frac{N-1}{2} F, \\ \psi_3 &= \left(E + \frac{N-1}{2} F\right)\left(E + \frac{N-3}{2} F\right) - 1, \end{aligned} \tag{5.3}$$

and so on. The amplitude $\psi_a = P_{a-1}(E)$ thus obtained is a polynomial with degree $a-1$ in E, dubbed a Lommel polynomial [52]. It also depends on N and F.

On the open chain of size N with Dirichlet boundary conditions, the energy levels E_n are the N zeros of the polynomial equation

$$\psi_{N+1} = P_N(E) = 0. \tag{5.4}$$

Furthermore, the IPR I_n of the eigenstate associated with energy E_n reads

$$I_n = \frac{\sum_{a=1}^N \psi_a^4}{\left(\sum_{a=1}^N \psi_a^2\right)^2} \tag{5.5}$$

in terms of the above amplitudes ψ_a. Hence I_n is a rational function of E_n, which also depends on N and F. As a consequence, the I_n are the N zeros of another polynomial equation of degree N, of the form

$$\Pi_N(I) = \sum_{k=0}^N \Pi_{N,k} I^k = 0. \tag{5.6}$$

The polynomial $\Pi_N(I)$ is the resultant of the algebraic elimination of E between the rational expressions (5.4) and (5.5). This observation simplifies considerably the calculation of T. This quantity is indeed the sum of the I_n (see (2.12)), and so

$$T = -\frac{\Pi_{N,N-1}}{\Pi_{N,N}}. \tag{5.7}$$

It is worth looking at the first few values of N.

- $N = 2$. The above formalism yields

$$P_2(E) = E^2 - 1 - \frac{F^2}{4}, \tag{5.8}$$

$$\Pi_2(I) = \left((4+F^2)I - 2 - F^2\right)^2. \tag{5.9}$$

The energy levels read

$$E_{1,2} = \pm\frac{1}{2}\sqrt{4+F^2}. \tag{5.10}$$

Both eigenstates have the same IPR

$$I_{1,2} = \frac{2+F^2}{4+F^2}. \tag{5.11}$$

We thus obtain

$$T = \frac{2(2+F^2)}{4+F^2}. \tag{5.12}$$

- $N = 3$. The above formalism yields

$$P_3(E) = E(E^2 - 2 - F^2), \tag{5.13}$$

$$\Pi_3(I) = \left((2+F^2)^2 I - 2 - F^4\right) \times \left(2(2+F^2)^2 I - 3 - 4F^2 - 2F^4\right)^2. \tag{5.14}$$

The energy levels read

$$E_{1,3} = \pm\sqrt{2+F^2}, \qquad E_2 = 0. \tag{5.15}$$

The corresponding IPR are

$$I_{1,3} = \frac{3 + 4F^2 + 2F^4}{2(2 + F^2)^2}, \qquad I_2 = \frac{2 + F^4}{(2 + F^2)^2}. \tag{5.16}$$

We thus obtain

$$T = \frac{5 + 4F^2 + 3F^4}{(2 + F^2)^2}. \tag{5.17}$$

• $N = 4$. Skipping details, we obtain

$$T = \frac{4(24 + 107F^2 + 91F^4 + 48F^6 + 36F^8)}{(1 + 2F^2)(5 + 2F^2)(16 + 12F^2 + 9F^4)}. \tag{5.18}$$

• $N = 5$. Skipping details, we obtain

$$T = \frac{\mathcal{N}_5(F)}{(3 + 4F^2 + 4F^4)^2(4 + 24F^2 + 9F^4)}, \tag{5.19}$$

with

$$\begin{aligned}\mathcal{N}_5(F) = 2(24 &+ 206F^2 + 615F^4 + 1676F^6 \\ &+ 700F^8 + 528F^{10} + 360F^{12}).\end{aligned} \tag{5.20}$$

The following observations can be made at this stage. The quantity T is a rational even function of the applied field F, whose complexity grows rapidly with N. Its degree in F reads $d_N = N^2/2$ if N is even, and $d_N = (N^2 - 1)/2$ if N is odd.

In the small-field limit, we have

$$T = T^{(0)} + T^{(2)}F^2 + \cdots \tag{5.21}$$

The first term is the known value of T for a free tight-binding particle [7], i.e.,

$$T^{(0)} = \begin{cases} \dfrac{3N}{2(N+1)} & (N \text{ even}), \\ \dfrac{3N+1}{2(N+1)} & (N \text{ odd}), \end{cases} \tag{5.22}$$

which saturates to the finite limit

$$T^{(0)} = \frac{3}{2} \tag{5.23}$$

for large system sizes. The coefficient $T^{(2)}$ will be calculated in section 5.2 for all N by means of perturbation theory (see (5.34), (5.35)).

In the large-field limit, T obeys a linear-plus-constant growth of the form

$$T \approx NI(F) + J(F), \tag{5.24}$$

asserting the poor equilibration properties characteristic of a localized regime, with

$$I(F) = 1 - \frac{4}{F^2} + \frac{9}{F^4} - \frac{100}{9F^6} + \frac{1225}{144F^8} + \cdots, \tag{5.25}$$

$$J(F) = \frac{4}{F^2} - \frac{2}{F^4} - \frac{104}{3F^6} + \frac{15943}{108F^8} + \cdots \tag{5.26}$$

As N increases, more and more terms of the above asymptotic expansions stabilize. This localized regime will be further investigated in sections 5.4 and 5.6.

5.2. Perturbation theory

The goal of this section is to determine the coefficient $T^{(2)}$ of the expansion (5.21) by means of second-order perturbation theory. The derivation follows the lines of section 5.1 of Reference [7], devoted to the case of a weak diagonal random potential.

In the absence of an electric field, the energy eigenvalues of a free tight-binding particle [7] read

$$E_n = 2\cos\frac{n\pi}{N+1} \tag{5.27}$$

($n = 1, \ldots, N$). The corresponding normalized eigenstates are

$$\langle a|n\rangle = \sqrt{\frac{2}{N+1}}\,\sin\frac{an\pi}{N+1}. \tag{5.28}$$

Their IPR read

$$I_n = \frac{1}{2(N+1)}\left(3 + \delta_{n,\frac{1}{2}(N+1)}\right). \tag{5.29}$$

For odd sizes N, the IPR of the central eigenstate at zero energy, with number $n = \frac{1}{2}(N+1)$, is enhanced by a factor 4/3. The expression (5.22) can be recovered by summing (5.29) over n.

In the presence of an electric field, the un-normalized nth eigenstate reads

$$|n\rangle_F = |n\rangle - F\sum_m B_{nm}|m\rangle + F^2\sum_{m\neq n} C_{nm}|m\rangle + \cdots, \tag{5.30}$$

with

$$B_{nm} = \frac{\langle m|W|n\rangle}{E_n - E_m}, \quad C_{nm} = \frac{1}{E_n - E_m}\sum_l \frac{\langle m|W|l\rangle\langle l|W|n\rangle}{E_n - E_l}, \tag{5.31}$$

where E_n and $|n\rangle$ are given by (5.27) and (5.28), while W is the operator

$$W = \sum_a \left(\frac{N+1}{2} - a\right)|a\rangle\langle a|, \tag{5.32}$$

where the quantity in the parentheses is the ratio V_a/F (see (5.2)). The property $\langle n|W|n\rangle = 0$ has been used in the derivation of (5.30).

Skipping details, let us mention that the expansion (5.30) yields after some algebra

$$\begin{aligned} T^{(2)} = {} & 6\sum_{a,n}\langle a|n\rangle^2\Big(\sum_m B_{nm}\langle a|m\rangle\Big)^2 \\ & + 4\sum_{a,n}\langle a|n\rangle^3\sum_{m\neq n} C_{nm}\langle a|m\rangle - 2\sum_{a,n}\langle a|n\rangle^4\sum_m B_{nm}^2. \end{aligned} \tag{5.33}$$

The final step of the derivation, i.e., the evaluation of the above sums, could not be done by analytical means. We have instead used the following trick. We know from the general approach of section 5.1 that $T^{(2)}$ is a rational number. A numerical evaluation of (5.33) with very high accuracy ($N = 400$ can be reached in one minute of CPU time) reveals that the denominator of $T^{(2)}$ is a divisor of $140(N+1)$ if N is even, and of $105(N+1)$ if N is odd. This serendipitous situation allows one to 'guess' the following exact closed-form expressions:

• *N even:*

$$T^{(2)} = \frac{N(N+2)(2N^4 + 8N^3 + 91N^2 + 166N + 153)}{10080(N+1)}. \tag{5.34}$$

• *N odd:*

$$T^{(2)} = \frac{(N-1)(N+3)(4N^4+16N^3-121N^2-274N-525)}{20160(N+1)}. \quad (5.35)$$

Table 2 gives a list of the coefficients $T^{(0)}$ and $T^{(2)}$ entering the expansion (5.21), up to $N = 10$. The results up to $N = 5$ agree with the expansions of the exact expressions (5.12)–(5.19). The coefficient $T^{(2)}$ turns out to be negative for $N = 3$ and $N = 5$, resulting in a non-monotonic dependence of T on the applied field F.

N	1	2	3	4	5	6	7	8	9	10
$T^{(0)}$	1	1	$\frac{5}{4}$	$\frac{6}{5}$	$\frac{4}{3}$	$\frac{9}{7}$	$\frac{11}{8}$	$\frac{4}{3}$	$\frac{7}{5}$	$\frac{15}{11}$
$T^{(2)}$	0	$\frac{1}{4}$	$-\frac{1}{4}$	$\frac{157}{100}$	$-\frac{1}{9}$	$\frac{583}{98}$	$\frac{5}{2}$	$\frac{311}{18}$	$\frac{299}{25}$	$\frac{1853}{44}$

Table 2. Coefficients $T^{(0)}$ and $T^{(2)}$ entering the expansion (5.21) of T, up to $N = 10$.

For large system sizes, the expansion (5.21) becomes

$$T \approx \frac{3}{2} + \frac{N^5F^2}{5040} + \cdots \quad (5.36)$$

We shall come back to this result in section 5.5 (see (5.82)).

5.3. Wannier-Stark spectrum on the infinite chain

The problem of a tight-binding particle on the infinite electrified chain has been studied long ago [45, 46, 47, 48, 49, 50]. The energy spectrum is an infinite Wannier-Stark ladder of the form $E_k = kF$, forgetting about the constant offset $(N + 1)/2$ in (5.1).

5.3.1. Spatial structure of Wannier-Stark states. The central Wannier-Stark state with energy

$$E_0 = 0 \quad (5.37)$$

is described by the normalized wavefunction

$$\psi_a = J_a(2/F), \quad (5.38)$$

where J_a is the Bessel function. We have $\psi_{-a} = (-1)^a\psi_a$, so that the probabilities ψ_a^2 are symmetric around the origin. All the other states are obtained from the above central one by translations along the chain. The state with energy

$$E_k = kF \quad (5.39)$$

is described by the wavefunction

$$\psi_a = J_{a-k}(2/F) \quad (5.40)$$

centered at site k.

There is a formal identity between the wavefunction (5.38) describing the central stationary Wannier-Stark state on the electrified chain and the time-dependent wavefunction [57, 58]

$$\psi_a(t) = \mathrm{i}^{-a}J_a(2t), \quad (5.41)$$

describing the ballistic spreading of a quantum walker modelled as a free tight-binding particle launched at the origin at time $t = 0$, with time t playing the role of the inverse field $1/F$, in our reduced units.

The regime of most physical interest is that of a small electric field. The square wavefunction of the central Wannier-Stark state is shown in figure 4 for $F = 0.02$. We summarize here for future use its behavior in various regions in the small-field regime. The following estimates stemming from the theory of Bessel functions [41, 59] can be recovered by semi-classical techniques based on the saddle-point method, as described in the physics literature [57, 58].

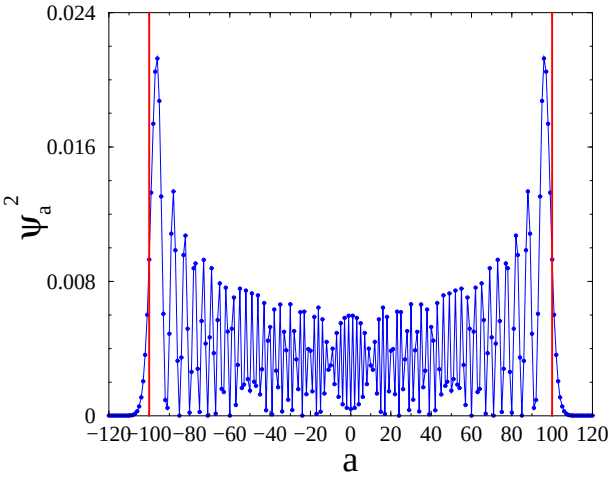

Figure 4. Square wavefunction ψ_a^2 of the central Wannier-Stark state against position a, for an electric field $F = 0.02$. Vertical lines show the nominal positions of the peaks in the transition regions ($a = \pm 100$).

Allowed region ($|aF| < 2$). The wavefunction only takes appreciable values in an allowed region extending up to a distance $2/F$ on either side of the origin. The size of the allowed region,

$$L(F) = 4/F, \tag{5.42}$$

plays the role of a localization length. More precisely, setting

$$aF = 2\cos\theta \qquad (0 < \theta < \pi), \tag{5.43}$$

we have

$$\psi_a \approx \left(\frac{F}{\pi \sin\theta}\right)^{1/2} \cos\left(\frac{2}{F}\left(\sin\theta - \theta\cos\theta\right) - \frac{\pi}{4}\right). \tag{5.44}$$

The allowed region is limited by two transition regions, located symmetrically near $a = \pm L(F)/2 = \pm 2/F$, corresponding to $\theta \to 0$ and $\theta \to \pi$.

Transition regions ($|aF| \approx 2$). In the transition regions at the endpoints of the allowed region, the wavefunction exhibit sharp peaks. In the right transition region, setting

$$aF = 2 + zF^{2/3}, \tag{5.45}$$

we have

$$\psi_a \approx F^{1/3}\mathrm{Ai}(z), \tag{5.46}$$

where $\mathrm{Ai}(z)$ is the Airy function. The width of the transition regions,

$$\lambda(F) \sim F^{-1/3}, \tag{5.47}$$

provides a second length scale which diverges in the small-field regime, albeit much less rapidly that $L(F)$ (see (5.42)).

Forbidden regions ($|aF| > 2$). The wavefunction falls off essentially exponentially fast in the forbidden regions. In the right forbidden region, setting

$$aF = 2\cosh\mu \qquad (\mu > 0), \tag{5.48}$$

we have

$$\psi_a \approx \left(\frac{F}{4\pi\sinh\mu}\right)^{1/2} \exp\left(-\frac{2}{F}\left(\mu\cosh\mu - \sinh\mu\right)\right). \tag{5.49}$$

5.3.2. IPR of Wannier-Stark states. All Wannier-Stark states have the common IPR

$$I(F) = \sum_a J_a^4(2/F). \tag{5.50}$$

This quantity was already investigated [57] in the context of the time-dependent wavefunction (5.41). It has also attracted some attention in the mathematical literature (see [60, 61] and references therein).

In the large-field regime ($F \gg 1$), the central Wannier-Stark state is very tightly localized near the origin. The amplitudes ψ_a indeed fall off as

$$\psi_a \approx \frac{1}{a!\,F^a} \qquad (a > 0). \tag{5.51}$$

The expansion (5.25) of $I(F)$ can therefore be recovered easily. An all-order asymptotic expansion can be derived by means of the following expression of the Mellin transform [57]:

$$\begin{aligned} M(s) &= \int_0^\infty F^{-s-1}\, I(F)\,\mathrm{d}F \\ &= \frac{\Gamma(s)}{2^{3s}\pi^{3/2}} \cos\frac{s\pi}{2} \left(\frac{\Gamma\left(\frac{1-s}{2}\right)}{\Gamma\left(\frac{2-s}{2}\right)}\right)^3 \qquad (0 < \mathrm{Re}\ s < 1). \end{aligned} \tag{5.52}$$

Summing the contributions of the simple poles at $s = -2, -4, \ldots$, we obtain

$$I(F) = \sum_{k\geq 0} \frac{(-1)^k (2k)!^2}{k!^6\, F^{2k}}. \tag{5.53}$$

The above result can be recovered by using the expression of $I(F)$ in terms of a hypergeometric function [60, 61]:

$$I(F) = {}_2\mathrm{F}_3\left(\frac{1}{2}, \frac{1}{2}; 1, 1, 1; -\frac{16}{F^2}\right). \tag{5.54}$$

In the small-field regime, we have

$$I(F) = \frac{F}{2\pi^2} \ln \frac{64 \mathrm{e}^{\gamma}}{F} + \frac{F^{3/2}}{16\sqrt{\pi}} \sin(8/F - \pi/4) + \cdots \tag{5.55}$$

The first term of the above expression exhibits a logarithmic correction, stemming from the double pole of $M(s)$ at $s = 1$, with respect to the leading scaling $I(F) \sim 1/L(F) \sim F$. The presence of this logarithmic correction to scaling was already emphasized in the time-dependent problem [57], where it was put in perspective with the following phenomenon dubbed bifractality. The generalized IPR

$$I^{(q)}(F) = \sum_a |J_a(2/F)|^{2q}, \tag{5.56}$$

with $q > 0$ arbitrary, exhibits an anomalous scaling behavior as $F \to 0^+$, of the form

$$I^{(q)}(F) \sim F^{\tau(q)}, \tag{5.57}$$

with

$$\tau(q) = \begin{cases} q - 1 & (q < 2), \\ \dfrac{2q-1}{3} & (q > 2). \end{cases} \tag{5.58}$$

The usual IPR $I(F)$ corresponds to $q = 2$, i.e., precisely the break point between both branches of the above bifractal spectrum, where the generalized IPR is respectively dominated by the allowed region (for $q < 2$) and by the transition regions (for $q > 2$).

The subleading oscillatory contribution in (5.55), whose derivation requires more sophisticated techniques [61], results in a non-monotonic behavior of the IPR $I(F)$ as a function of the field F.

5.4. Main features of the IPR I_n and of T

In this section we provide a picture of the salient features of the IPR I_n of the various eigenstates, and of their sum T.

Figure 5 shows the IPR I_n against the energy E_n for all eigenstates of finite chains of various lengths ranging from $N = 8$ to 100. The applied field reads $F = 0.1$, so that the localization length is $L(F) = 40$. The horizontal line shows the value $I(F) = 0.035\,222\ldots$ of the IPR of Wannier-Stark states. The IPR I_n have been evaluated by means of a direct numerical diagonalization of the Hamiltonian matrix $\mathcal{H}$. The symmetry of the plot with respect to $E = 0$ is manifest. As N increases, the IPR of the few first (or last) eigenstates converge very fast to well-defined limiting values. In the small-field regime, these limits will be shown to scale as $F^{1/3}$ (see (5.70)). They are therefore much larger than the IPR $I(F)$ of Wannier-Stark states, which is proportional to F, with a logarithmic correction (see (5.55)). In the localized regime, i.e., for sample sizes N larger than the localization length $L(F)$, there are approximately $N - L(F)$ bulk states in the central part of the energy spectrum:

$$|E| < \tfrac{1}{2}NF - 2. \tag{5.59}$$

These eigenstates are exponentially close to the Wannier-Stark states whose allowed region is entirely contained in the sample (see e.g. [51, 52, 55]). Their IPR I_n is therefore very close to $I(F)$. The remaining eigenstates are edge states, living near either boundary of the system, whose energies lie in the wings of the spectrum:

$$\tfrac{1}{2}NF - 2 < |E| < \tfrac{1}{2}NF + 2. \tag{5.60}$$

Their IPR vary in a broad range between $I(F)$ and $F^{1/3}$. On shorter samples, whose length N is smaller than the localization length $L(F)$, the distinction between bulk and edge states looses its meaning. All the IPR I_n are larger than $I(F)$ and manifest a rather irregular dependence on the state number n. This is exemplified by the data for system sizes $N = 8$ to 20 in figure 5.

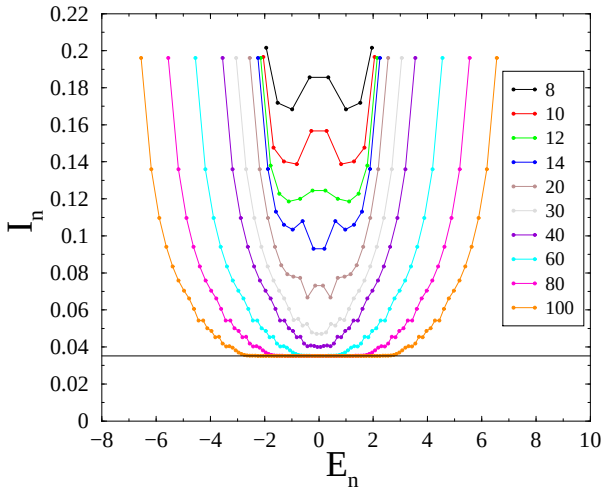

Figure 5. IPR I_n against energy E_n for all eigenstates of finite chains of various lengths N, for an applied field $F = 0.1$. Horizontal line: $I(0.1) = 0.035\,222\ldots$

The above picture substantiates the asymptotic linear-plus-constant growth of T with the system size N, already advocated in (5.24):

$$T \approx NI(F) + J(F). \tag{5.61}$$

This estimate holds not only for large fields, but all over the localized regime, defined by the inequality $N > L(F)$, i.e., $NF > 4$. The slope $I(F)$ is the IPR of Wannier-Stark states (see (5.50)). The offset $J(F)$ somehow encodes the contributions of all edge states. Its exact value is not known for arbitrary values of the field F. It can be noticed that the coefficients of its large-field expansion (5.26) do not exhibit any obvious regularity. The quantity $J(F)$ will be investigated in section 5.6 in the small-field regime (see (5.106)).

Figure 6 shows the ratio T/N against F for several system sizes N. The lowest black line shows the IPR $I(F)$, corresponding to the $N \to \infty$ limit of T/N, according to (5.61). The data for finite N converge smoothly to that limit, for any fixed non-zero value of the electric field F.

The quantitative analysis of the IPR I_n and of their sum T in the small-field regime will require some special care. Two different characteristic lengths indeed diverge in the $F \to 0^+$ limit, namely $L(F) \sim 1/F$ (see (5.42)) and $\lambda(F) \sim 1/F^{1/3}$ (see (5.47)). Each of these diverging lengths is responsible for the occurrence of a non-trivial scaling regime (see sections 5.5 and 5.6).

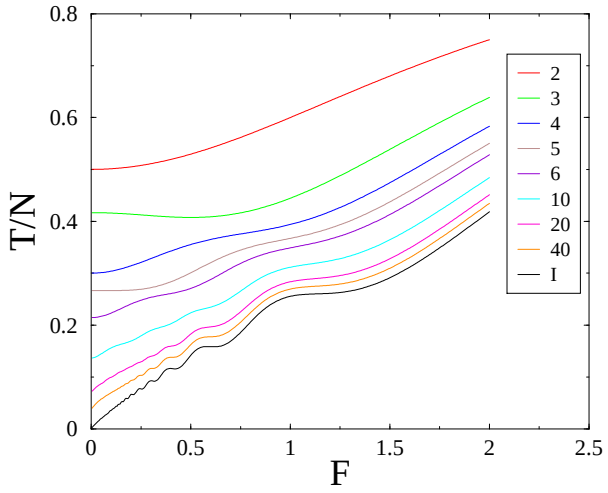

Figure 6. Ratio T/N against F for several system sizes N. Lowest black line: IPR $I(F)$, corresponding to $N \to \infty$.

5.5. Airy scaling regime ($N \sim \lambda(F) \sim 1/F^{1/3}$)

This section is devoted to the regime where the system size N and the size $\lambda(F)$ of the transition regions (see (5.47)) are large and comparable. We introduce the scaling variable

$$x = NF^{1/3}, \tag{5.62}$$

proportional to the ratio $N/\lambda(F)$. Since the wavefunction of the Wannier-Stark states in the transition regions is an Airy function (see (5.46)), we dub this regime the Airy scaling regime.

5.5.1. Extremal edge states. Let us first investigate the extremal edge states on a very large sample, with energies near the left edge of the spectrum ($E \approx -\frac{1}{2}NF - 2$). A direct approach goes as follows (see e.g. [53, 54]). Setting

$$\chi_a = (-1)^a \psi_a, \tag{5.63}$$

and replacing $N+1$ by N in the offset of the electrostatic potential, the tight-binding equation (5.1) becomes

$$\chi_{a+1} + \chi_{a-1} = \left(aF - \frac{NF}{2} - E \right) \chi_a. \tag{5.64}$$

Using a continuum description, this reads

$$\frac{\mathrm{d}^2\chi}{\mathrm{d}a^2} \approx (aF + \mathcal{E})\chi, \tag{5.65}$$

with

$$\mathcal{E} = -\frac{NF}{2} - E - 2, \tag{5.66}$$

and with the boundary conditions that χ vanishes for $a = 0$ and $a \to +\infty$. Then, setting

$$a = (z + c)F^{-1/3}, \qquad \mathcal{E} = -cF^{2/3}, \tag{5.67}$$

equation (5.65) boils down to Airy's equation

$$\frac{\mathrm{d}^2\chi}{\mathrm{d}z^2} = z\chi, \tag{5.68}$$

whose solution decaying as $z \to +\infty$ is $\chi(z) = \mathrm{Ai}(z)$.

The extremal edge states are quantized by the Dirichlet boundary condition at $a = 0$. The latter requires $c = c_n$, where $-c_n$ are the zeros of the Airy function ($n = 1, 2, \ldots$). These zeros are real and negative, and so $c_n > 0$. The extremal edge states on a very large sample therefore have energies

$$E_n \approx -\frac{NF}{2} - 2 + c_n F^{2/3}. \tag{5.69}$$

The IPR of these states read

$$I_n \approx a_n F^{1/3}, \tag{5.70}$$

with

$$a_n = \frac{\mu_4(c_n)}{\mu_2^2(c_n)} \tag{5.71}$$

and

$$\mu_m(c) = \int_{-c}^{+\infty} \mathrm{Ai}^m(z)\,\mathrm{d}z. \tag{5.72}$$

Numerical values of the first c_n and a_n are given in table 3.

n	c_n	a_n
1	2.338 107	0.417 433
2	4.087 949	0.291 084
3	5.520 559	0.236 155
4	6.786 708	0.203 572
5	7.944 133	0.181 374

Table 3. Numerical values of the first c_n, the opposites of the zeros of the Airy function, entering (5.69), and of the associated amplitudes a_n entering (5.70).

The above results can be made more explicit for large n, which will turn out to be the regime of interest. The asymptotic behavior of the Airy function

$$\mathrm{Ai}(z) \approx \frac{1}{\sqrt{\pi}|z|^{1/4}} \sin\left(\frac{2}{3}|z|^{3/2} + \frac{\pi}{4}\right) \qquad (z \to -\infty) \tag{5.73}$$

implies

$$c_n \approx \left(\frac{3\pi n}{2}\right)^{2/3}. \tag{5.74}$$

Then, for large c, averaging first the powers of the rapidly varying sine function, we obtain

$$\mu_2(c) \approx \frac{1}{2}\int_{-c}^{0} \frac{\mathrm{d}z}{\pi|z|^{1/2}} \approx \frac{\sqrt{c}}{\pi}, \tag{5.75}$$

$$\mu_4(c) \approx \frac{3}{8}\int_{-c}^{-c_0} \frac{\mathrm{d}z}{\pi^2|z|} \approx \frac{3}{8\pi^2}\ln\frac{c}{c_0}. \tag{5.76}$$

The finite part c_0 of the logarithm has been evaluated by more sophisticated techniques [62] yielding

$$\mu_4(c) \approx \frac{3}{8\pi^2}\ln(4\mathrm{e}^{2\gamma/3}c), \tag{5.77}$$

where γ is again Euler's constant. We thus obtain the estimate

$$a_n \approx \frac{1}{4}\left(\frac{3\pi n}{2}\right)^{-2/3}\ln(12\pi\mathrm{e}^{\gamma}n). \tag{5.78}$$

5.5.2. Scaling behavior of T. Let us come back to the evaluation of the sum T for large but finite systems in the Airy scaling regime.

The IPR I_n of the nth eigenstate scales as

$$I_n \approx \frac{1}{N}\phi_n(x), \tag{5.79}$$

with

$$\phi_n(x) \approx \begin{cases} \dfrac{3}{2} & (x \to 0), \\ a_n x & (x \to \infty). \end{cases} \tag{5.80}$$

The above estimates respectively match (5.29) and (5.70).

As a consequence, T obeys a scaling law

$$T \approx T^{(0)} + \frac{1}{N}\,\Phi(x) \tag{5.81}$$

of the very same form as (1.1), corresponding to a particle in a weak disordered potential [7], albeit with a different scaling variable x, and a different function $\Phi(x)$. The first term is the value of T for a free particle, given by (5.22), and so we have $\Phi(0) = 0$. The following observation made in [7] also applies to the present situation. Had we chosen the limit value (5.23) for $T^{(0)}$ as the first term in (5.81), instead of the exact expression (5.22) for finite N, the scaling function $\Phi(x)$ would have acquired a finite offset depending on the parity of N, i.e., $\Phi(0) = -3/2$ (resp. $\Phi(0) = -1$) for N even (resp. N odd).

When the scaling variable x is small, the outcome (5.36) of perturbation theory implies

$$\Phi(x) \approx \frac{x^6}{5040} \qquad (x \to 0). \tag{5.82}$$

The asymptotic behavior of the scaling function $\Phi(x)$ at large x can be estimated as follows. The crossover between both estimates entering (5.80) remains steep, in the sense that it does not broaden out as the state number n gets larger and larger. The sum T can therefore be estimated as

$$T \approx \frac{2}{N}\sum_{n=1}^{N/2} \max\left(\frac{3}{2},\, a_n x\right). \tag{5.83}$$

Using the expression (5.78) for the amplitudes a_n, we obtain after some algebra

$$\Phi(x) \approx 6 n_c(x), \tag{5.84}$$

where $n_c(x)$ is the value of n such that both arguments of the max function entering (5.83) coincide. To leading order in $\ln x \gg 1$, we have

$$n_c(x) \approx \frac{(x \ln x)^{3/2}}{12\pi}, \tag{5.85}$$

and so

$$\Phi(x) \approx \frac{(x \ln x)^{3/2}}{2\pi} \qquad (x \to \infty). \tag{5.86}$$

Figure 7 shows a log-log plot of the ratio $\Phi(x)/x^4$ against the scaling variable x. This ratio has been chosen in order to better reveal the structure of the scaling function $\Phi(x)$. Color lines show data pertaining to system sizes 100, 200 and 400. The straight line to the left shows the power-law result (5.82) stemming from perturbation theory. The line to the right shows the estimate (5.86). The data exhibit a very good convergence to the scaling function $\Phi(x)$, as well as a good agreement with both analytical predictions. Small oscillatory corrections are however visible at very high x.

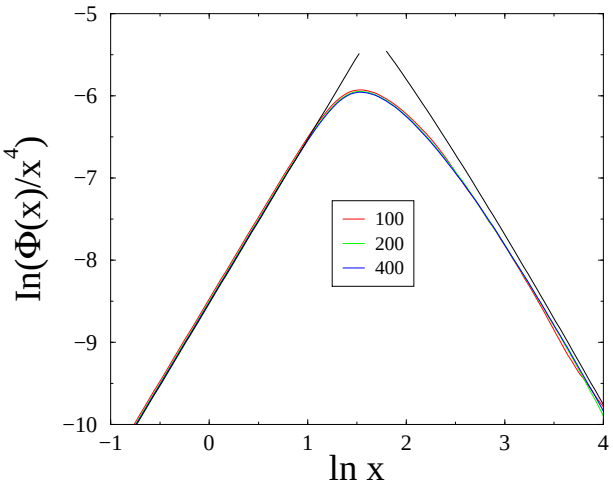

Figure 7. Log-log plot of the ratio $\Phi(x)/x^4$ against the scaling variable x. Color lines: data pertaining to system sizes 100, 200 and 400. Straight line to the left: power-law result (5.82). Line to the right: estimate (5.86).

5.6. Bessel scaling regime ($N \sim L(F) \sim 1/F$)

This section is devoted to the regime where the system size N and the localization length $L(F)$ (see (5.42)) are large and comparable. We introduce the scaling variable

$$y = NF, \tag{5.87}$$

proportional to the ratio $N/L(F)$, and dub this regime the Bessel scaling regime.

5.6.1. Generic edge states. Let us first investigate the generic edge states on a very large sample in the localized regime ($y > 4$), considering the left edge for definiteness. These edge states are very well described by the restriction of the Wannier-stark states (5.40), i.e.,

$$\psi_a = J_{a-k}(2/F), \tag{5.88}$$

to a part of their allowed region. The allowed region of the above wavefunction is $k - 2/F < a < k + 2/F$. Left edge states therefore correspond to the range $-2/F < k < 2/F$, i.e., $-\frac{1}{2}y - 2 < E < -\frac{1}{2}y + 2$, in agreement with (5.60).

The above edge states are quantized by the Dirichlet boundary condition $\psi_0 = 0$. Setting

$$k = -\frac{2\cos\alpha}{F}, \qquad E = -\frac{y}{2} - 2\cos\alpha, \tag{5.89}$$

the expression (5.44) of the wavefunction in the allowed region yields the quantization condition

$$\sin\alpha_n - \alpha_n \cos\alpha_n \approx \frac{\pi n F}{2}. \tag{5.90}$$

As the angle α increases from 0 to π, the edge state number n ranges from 1 to $n_{\rm edge}$, where

$$n_{\rm edge} = \frac{2}{F} = \frac{L(F)}{2} \tag{5.91}$$

is our estimate for the number of edge states in each wing of the spectrum in the small-field regime. The quantization condition (5.90) yields the density of states

$$\rho(\alpha) = \frac{2}{\pi F}\,\alpha \sin\alpha, \tag{5.92}$$

normalized as

$$\int_0^\pi \rho(\alpha)\,{\rm d}\alpha = n_{\rm edge}. \tag{5.93}$$

The IPR of the above edge states read

$$I_n = \frac{S_{4,n}}{S_{2,n}^2}, \tag{5.94}$$

with

$$S_{m,n} = \sum_{a\geq 1} \psi_{a,n}^m, \tag{5.95}$$

and $\psi_{a,n}$ is given by (5.88), together with the quantization condition (5.90). The sums $S_{m,n}$ can be estimated by using the expression (5.44) of the wavefunction in the allowed region, averaging first the powers of the sine function, and transforming the sums over a into integrals over θ in the range $0 < \theta < \alpha_n$, according to (5.43). We thus obtain

$$S_{2,n} \approx \frac{1}{2}\cdot\frac{2}{\pi}\int_0^{\alpha_n} {\rm d}\theta = \frac{\alpha_n}{\pi}, \tag{5.96}$$

$$S_{4,n} \approx \frac{3}{8}\cdot\frac{2F}{\pi^2}\int_\varepsilon^{\alpha_n} \frac{{\rm d}\theta}{\sin\theta} = \frac{3F}{4\pi^2}\ln\left(\frac{2}{\varepsilon}\tan\frac{\alpha_n}{2}\right), \tag{5.97}$$

and so

$$I_n \approx \frac{3F}{4\alpha_n^2}\ln\left(\frac{2}{\varepsilon}\tan\frac{\alpha_n}{2}\right). \tag{5.98}$$

The cutoff ε is independent of the state number n. It can therefore be determined by matching the Airy and Bessel regimes. For $n \ll n_{\rm edge}$, i.e., $nF \ll 1$, (5.90) reads

$$\alpha_n \approx \left(\frac{3\pi nF}{2}\right)^{1/3}. \tag{5.99}$$

Identifying the expressions (5.70), (5.78) in the Airy regime and (5.98), (5.99) in the Bessel regime yields

$$\varepsilon = \left(\frac{F}{8\mathrm{e}^{\gamma}}\right)^{1/3}. \tag{5.100}$$

We are thus left with the estimate

$$I_n \approx \mathcal{I}(F,\alpha_n) = \frac{F}{4\alpha_n^2}\ln\left(\frac{64\mathrm{e}^{\gamma}}{F}\tan^3\frac{\alpha_n}{2}\right). \tag{5.101}$$

5.6.2. Scaling behavior of T. Let us come back to the evaluation of the sum T for finite systems in the Bessel scaling regime.

• $y > 4$. Consider first the simple situation of samples in the localized regime, such that $N > L(F)$, i.e., $y > 4$. As already discussed in section 5.4, there are $N - 2n_{\rm edge} = N - L(F) = (y-4)/F$ bulk states, whose IPR essentially coincide with $I(F)$, and $2n_{\rm edge} = L(F) = 4/F$ edge states, whose IPR vary according to (5.101). We thus obtain

$$T \approx (y-4)\frac{I(F)}{F} + T_{\rm edge}, \tag{5.102}$$

where the contribution of all edge states reads

$$T_{\rm edge} \approx 2\int_0^{\pi} \rho(\alpha)\,\mathcal{I}(F,\alpha)\,\mathrm{d}\alpha = A\ln\frac{64\mathrm{e}^{\gamma}}{F} + 3B, \tag{5.103}$$

with

$$A = \frac{1}{\pi}\int_0^{\pi}\frac{\sin\alpha}{\alpha}\,\mathrm{d}\alpha = \frac{\mathrm{Si}(\pi)}{\pi} = 0.589\,489\ldots, \tag{5.104}$$

$$B = \frac{1}{\pi}\int_0^{\pi}\frac{\sin\alpha}{\alpha}\,\ln\tan\frac{\alpha}{2}\,\mathrm{d}\alpha = -0.462\,288\ldots \tag{5.105}$$

The result (5.102) has the expected linear-plus-constant form (5.24), (5.61). It yields the following estimate for the offset $J(F)$ in the small-field regime:

$$J(F) \approx \left(A - \frac{2}{\pi^2}\right)\ln\frac{64\mathrm{e}^{\gamma}}{F} + 3B. \tag{5.106}$$

Finally, (5.102) can be recast as

$$T \approx U(y)\ln\frac{1}{F} + V(y), \tag{5.107}$$

with

$$U(y) = \frac{y-4}{2\pi^2} + A, \tag{5.108}$$

$$V(y) = \left(\frac{y-4}{2\pi^2} + A\right)\ln(64\mathrm{e}^{\gamma}) + 3B. \tag{5.109}$$

• $y < 4$. Consider now shorter samples, such that $N < L(F)$, i.e., $y < 4$. As discussed in section 5.4, there is no clear-cut distinction between bulk and edge states in this situation. As a consequence, the formula (5.101) for the IPR of edge states is not sufficient to derive an estimate of T for $y < 4$. We nevertheless hypothesize that T still obeys a logarithmic scaling law in F of the form (5.107), even though the amplitudes $U(y)$ and $V(y)$ cannot be predicted analytically. Figure 8 presents numerical results for these amplitudes. For each value of y, T has been calculated for 15 roughly equidistant system sizes N on a logarithmic scale between $N = 10$ and $N = 5000$. These values of T obey accurately the logarithmic dependence on F, i.e., on $N = y/F$, hypothesized in the scaling form (5.107). The resulting estimates for $U(y)$ and $V(y)$ are shown as symbols in both panels of figure 8. Black lines show fits of the form $U(y) = (u_1 \ln y + u_2)\sqrt{y} + (u_3 \ln y + u_4)y$ and $V(y) = 3/2 + (v_1 \ln y + v_2)\sqrt{y} + (v_3 \ln y + v_4)y$. The form of these fits is freely inspired by the expected crossover at small y with the estimate (5.86) for large x in the Airy regime, i.e.,

$$T \approx \frac{3}{2} + \frac{\sqrt{y}}{2\pi}\left(\ln \frac{y}{F^{2/3}}\right)^{3/2}. \tag{5.110}$$

In any case, the proposed fits describe the data accurately. Finally, the blue straight lines show the analytical results (5.108), (5.109) for $y > 4$. The data suggest that the functions $U(y)$ and $V(y)$ are continuous at $y = 4$, as well as their first derivatives.

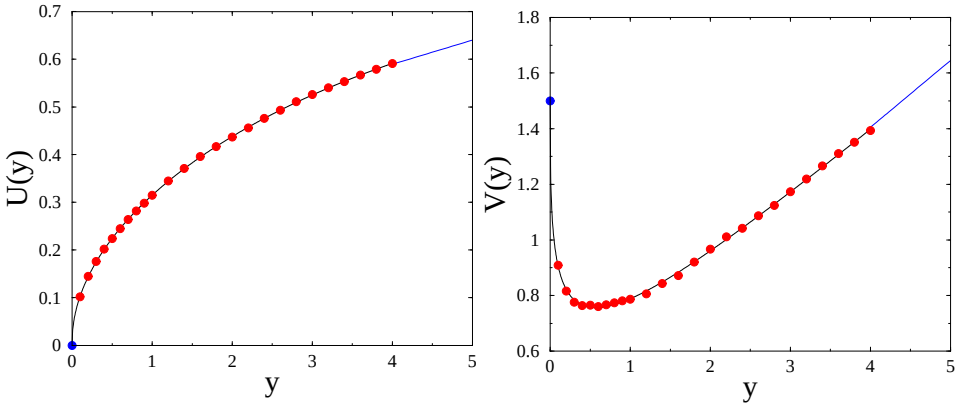

Figure 8. Amplitudes $U(y)$ (left) and $V(y)$ (right) entering the scaling formula (5.107) for T. Red symbols: numerical data for $y < 4$. Black lines: fits to these data (see text). Blue straight lines: analytical results (5.108), (5.109) for $y > 4$. Blue symbols: values $U(0) = 0$ and $V(0) = 3/2$.

6. Discussion

A novel way of investigating equilibration – or lack of equilibration – in small isolated quantum systems has been put forward recently [7]. The key quantity of that approach is the trace T of the matrix Q of asymptotic transition probabilities in some preferential basis chosen once for all. The quantity T is also the sum of the inverse participation

ratios of all eigenstates of the Hamiltonian in the same basis. It provides a measure of the degree of equilibration of the system if launched from a typical basis state of the preferential basis. It may vary between $T_{\min} = 1$ and $T_{\max} = N$, the dimension of the Hilbert space; the larger T, the poorer the equilibration.

The different physical systems investigated both in [7] and in the present work provide useful examples allowing one to get an extensive understanding of the behavior of the quantity T. Quantum systems whose dynamics is governed by a generic Hamiltonian exhibit good typical equilibration properties, so that T saturates to a non-trivial limit for large N. This limit is however always found to be larger than $T_{\min} = 1$. It equals $T^{(0)} = 3/2$ for a free tight-binding particle on a large open interval [7], and $T_{\rm U} = 2$ or $T_{\rm O} = 3$ for a random Hamiltonian whose distribution is invariant under the groups $\mathrm{U}(N)$ or $\mathrm{O}(N)$ (section 3).

An interesting situation is met when varying a system parameter through some scaling regime induces a continuous transition from good to bad equilibration properties. Three different one-particle systems are known to exhibit such a crossover phenomenon, where T is found to obey non-trivial scaling behavior. For a spin S in a tilted magnetic field (section 4) making an angle θ with the preferred quantization axis, we have $T = T_{\max} = N$ for $\theta = 0$, while $T \sim \ln N$ for any fixed non-zero tilt angle θ. Both regimes are connected by the scaling laws (4.23), (4.24), with scaling variable $u = N\theta$. For a tight-binding particle on a finite open chain in a weak random potential [7], T obeys the scaling law recalled in the Introduction (see (1.1)), with scaling variable $x = Nw^{2/3}$, which describes the crossover between the finite value $T = T^{(0)} = 3/2$ of a free particle in the ballistic regime and the linear growth $T \approx NQ$ in the localized regime, testifying poor equilibration, with $Q \sim w^{4/3}$ for a weak disorder. For a tight-binding particle on a finite electrified chain (section 5), T obeys a similar but richer behavior in the situation where the applied field F is small, so that the localization length $L(F) = 4/F$ is large. The quantity T indeed exhibits two successive scaling laws describing the crossover between the ballistic regime and the insulating one, namely a first scaling law of the form (5.81) with scaling variable $x = NF^{1/3}$ in the so-called Airy scaling regime, followed by a second scaling law of the form (5.107) with scaling variable $y = NF$ in the so-called Bessel scaling regime.

The results on the XXZ spin chain [8] demonstrate that a transition from good to bad equilibration properties, in the sense of a change in the growth law of T, can be observed in a clean quantum many-body system which does not exhibit many-body localization. There, the transition is found to coincide with a thermodynamical phase transition, with $T \sim L$ in the gapless phase of the model ($|\Delta| < 1$), and $T \sim \exp(aL)$ in the gapped phase ($|\Delta| > 1$). It would be worth sorting out in a broader setting the connection between changes in the scaling behavior of the quantity T and various types of phase transitions, involving or not the appearance of many-body localized phases.

Acknowledgments

It is a pleasure to thank P Krapivsky, K Mallick and G Misguich for fruitful discussions, and especially V Pasquier for his interest in this work and for a careful reading of the manuscript.

References

[1] Cazalilla M A and Rigol M 2010 *New J. Phys.* **12** 055006
[2] Polkovnikov A, Sengupta K, Silva A and Vengalattore M 2011 *Rev. Mod. Phys.* **83** 863
[3] Eisert J, Friesdorf M and Gogolin C 2011 *Nature Phys.* **11** 124
[4] Nandkishore R and Huse D A 2015 *Annu. Rev. Cond. Mat. Phys.* **6** 15
[5] Gogolin C and Eisert J 2016 *Rep. Prog. Phys.* **79** 056001
[6] D'Alessio L, Kafri Y, Polkovnikov A and Rigol M 2016 *Adv. Phys.* **65** 239
[7] Luck J M 2016 *J. Phys. A* **49** 115303
[8] Misguich G, Pasquier V and Luck J M 2016 *Phys. Rev. B* **94** 155110
[9] Tsukerman E 2016 Preprint arXiv:1611.01806
[10] Reimann P 2008 *Phys. Rev. Lett.* **101** 190403
[11] Linden N, Popescu S, Short A J and Winter A 2009 *Phys. Rev. E* **79** 061103
[12] Linden N, Popescu S, Short A J and Winter A 2010 *New J. Phys.* **12** 055021
[13] Gogolin C, Müller M P and Eisert J 2011 *Phys. Rev. Lett.* **106** 040401
[14] Short A J 2011 *New J. Phys.* **13** 053009
[15] Ikeda T N and Ueda M 2015 *Phys. Rev. E* **92** 020102
[16] Bell R J, Dean P and Hibbins-Butler D C 1970 *J. Phys. C* **3** 2111
[17] Bell R J and Dean P 1970 *Discuss. Faraday Soc.* **50** 55
[18] Visscher W M 1972 *J. Non-Cryst. Sol.* **8-10** 477
[19] Thouless D J 1974 *Phys. Rep.* **13** 93
[20] Vourdas A 2004 *Rep. Prog. Phys.* **67** 267
[21] Kibler M R 2009 *J. Phys. A* **42** 353001
[22] Bengtsson I and Zyczkowski K 2017 Preprint arXiv:1701.07902
[23] Beenakker C W J 1997 *Rev. Mod. Phys.* **69** 731
[24] Guhr T, Müller-Groeling A and Weidenmüller H A 1998 *Phys. Rep.* **299** 189
[25] Mehta M L 2004 *Random Matrices* 3rd ed (New York: Academic Press)
[26] Akemann G, Baik P and di Francesco P (eds) 2011 *The Oxford Handbook of Random Matrix Theory* (Oxford: Oxford University Press)
[27] Ullah N 1964 *Nucl. Phys.* **58** 65
[28] Weingarten D 1978 *J. Math. Phys.* **19** 999
[29] Itzykson C and Zuber J B 1980 *J. Math. Phys.* **21** 411
[30] Samuel S 1980 *J. Math. Phys.* **21** 2695
[31] Drouffe J M and Zuber J B 1983 *Phys. Rep.* **102** 1
[32] Collins B 2003 *Int. Math. Res. Not.* **17** 953
[33] Collins B and Śnaidy P 2006 *Commun. Math. Phys.* **264** 773
[34] Aubert S and Lam C S 2003 *J. Math. Phys.* **44** 6112
[35] Braun D 2006 *J. Phys. A* **39** 14581
[36] Gorin T and López G V 2008 *J. Math. Phys.* **49** 013503
[37] Messiah A 1999 *Quantum Mechanics* (New York: Dover)
[38] Feynman R P, Leighton R and Sands M 2013 *The Feynman Lectures on Physics, Volume III* (California Institute of Technology) [Online edition]
[39] Edmonds A R 1974 *Angular Momentum in Quantum Mechanics* (Princeton: Princeton University Press)
[40] Rose M E 1995 *Elementary Theory of Angular Momentum* (New York: Dover)
[41] Erdélyi A 1953 *Higher Transcendental Functions (The Bateman Manuscript Project)* (New York: McGraw-Hill)
[42] Bailey W N 1938 *J. London Math. Soc.* **13** 8
[43] Maximon L C 1956 *Norske Vid. Selsk. Forh. Trondheim* **29** 82
[44] Zudilin W 2014 *Bull. Austral. Math. Soc.* **89** 125
[45] Katsura S, Hatta T and Morita A 1950 *Sci. Rep. Tohuku Imp. Univ. (Ser. I)* **34** 19
[46] Feuer P 1952 *Phys. Rev.* **88** 92
[47] Hacker K and Obermair G 1970 *Z. Phys.* **234** 1
[48] Wannier G H 1959 *Elements of Solid State Theory* (Cambridge: Cambridge University Press)
[49] Wannier G H 1960 *Phys. Rev.* **117** 432
[50] Wannier G H 1962 *Rev. Mod. Phys.* **34** 645
[51] Heinrichs J and Jones R O 1972 *J. Phys. C* **5** 2149
[52] Stey G C and Gusman G 1973 *J. Phys. C* **6** 650
[53] Saitoh M 1973 *J. Phys. C* **6** 3255
[54] Fukuyama H, Bari R A and Fogedby H C 1973 *Phys. Rev. B* **8** 5579
[55] Entin-Wohlman O 1974 *J. Phys. C* **7** 3354

[56] Berezhkovskii A M and Ovchinnikov A A 1978 *Phys. Stat. Sol. (b)* **85** 121
[57] de Toro Arias S and Luck J M 1998 *J. Phys. A* **31** 7699
[58] Krapivsky P L, Luck J M and Mallick K 2015 *J. Phys. A* **48** 475301
[59] Watson G N 1958 *A Treatise on the Theory of Bessel Functions* (Cambridge: Cambridge University Press)
[60] Stoyanov B J and Farrell R A 1987 *Math. Comput.* **49** 275
[61] Landau L J and Luswili N J 2001 *J. Comput. Appl. Math.* **132** 387
[62] Reid W H 1997 *Z. angew. Math. Phys.* **48** 656